

SIMULTANEOUS REGISTRATION AND LANDMARK DETECTION

Sarah L. Bond and Michael Brady*

Wolfson Medical Vision Laboratory, Oxford University, UK
{sarah,jmb}@robots.ox.ac.uk

ABSTRACT

We are developing a system for patient management in colorectal cancer, in which a difficult case of non-rigid registration, namely of pre- and post-therapy images, arises. Numerous non-rigid registration algorithms have been proposed in Medical Image Analysis, and we have applied several leading algorithms to our non-rigid registration problem; but with unpromising results. The fundamental reason appears to be that they lack with knowledge of the particular application. We propose a graphical representation of anatomical knowledge relevant for colorectal cancer, and of the ways in which this anatomy may be predicted to change as a result of chemo and radiotherapy. We show how we interleave this representation with an adaptive registration algorithm to make the non-rigid registration result both robust and accurate.

I. INTRODUCTION

A frequent patient management decision in colorectal cancer calls for the patient to undergo a course of neo-adjuvant chemotherapy, primarily to downstage a tumor, prior to surgical resection. This decision is usually based on small field of view T2-weighted MRI images [1], from which the tumor is first staged using the standard TNM scheme (T = primary tumor, N = lymph nodes, M = metastases) [2]. Following the course of chemotherapy, a second MRI is taken and assessed relative to that taken earlier, primarily to gauge changes in lymph node involvement, and tumour shrinking and invasion of the submucosa, surrounding muscle, muscularis propria subserosa or non-peritonealized perirectal tissues. This assessment requires that the MRI volume taken prior, be registered with that taken post chemotherapy. The intrinsic complexity of colorectal anatomy, substantial variations to normal anatomy as a consequence of cancer, postural differences during imaging, and, most especially the substantial anatomical (and physiological) changes wrought by chemotherapy, mean that this turns out to be a very difficult registration problem, with substantial local deformations.

Due to the large scale changes involved in the deformations, many state of the art non-rigid registration algorithms

still failed to give an acceptable registration result [3]. To improve the registration some prior knowledge needs to be incorporated, and this is often done using an initial segmentation. However using a segmentation on its own for the registration, although robust, is not inherently accurate. For an accurate registration, we would require a perfect segmentation, or else the errors in the segmentation can cause even greater errors in the registration. However it is impossible to achieve a perfect segmentation for the wide range of images that we are observing due to the vast differences in anatomy, size of patient, size of tumor etc.

It has recently been suggested that simultaneous segmentation and registration is a superior method of registering two images using the known segmented features within those images. Chen et al. [4] showed that by interleaving the segmentation and registration steps within a Bayesian framework, both the segmentation and registration results were improved. They were identifying tissue types in Contrast Enhanced Breast MRI images, whilst aligning the images that were taken over the course of 6 minutes. The images needed registering due to motion of the patient over this period of time. A maximum a-posteriori (MAP) estimation was used for the segmentation and registration stages, and a Markov Random Field was also incorporated as a noise reduction measure. The results showed a reduction in misclassification of pixels within the images.

The problem of aligning and segmenting contrast-enhanced breast images is however quite a different problem to that of aligning the Colorectal MR images, since the colorectal images are taken 6 months apart, and after extensive chemo and radiotherapy. As such the deformations are much greater and unpredictable, causing many generic, "off the shelf" registration algorithms to fail [3]. Although the problem of aligning the breast MR images is critical for diagnosis, the scale of the changes is much smaller, and the robustness problem is therefore less of an issue.

We have previously shown that incorporating shape knowledge will increase the robustness of the registration [3]. In this paper we show how we can incorporate the shape knowledge, or relational representation, into a simultaneous registration and landmark detection algorithm. Since we are not interested in segmenting every pixel in the image into a different class, but are only interested in key features in

*Thanks to EPSRC and GE Healthcare for funding.

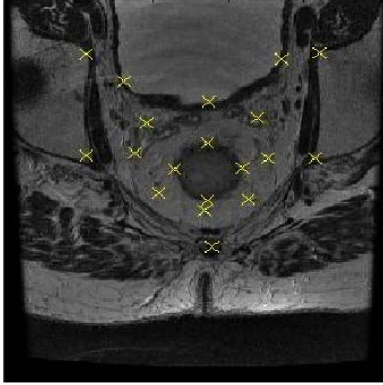


Fig. 1. Initial landmarks found on the images.

terms of the segmentation, we do not use the Bayesian MAP approach, but instead simply interleave landmark detection and registration steps within an adaptive registration framework.

II. SIMULTANEOUS LANDMARK DETECTION AND REGISTRATION

II-A. Initialization

An algorithm has already been implemented that finds landmark positions based on a relational representation of the anatomy visible within the images. These landmark points are features such as the colorectum, bone structures, mesorectum, and coccyx. They are found on the images using information about their appearance and positions. Full details of this method can be found in [5]. The landmarks themselves can be seen in Fig. 1. The method used gives a robust anatomical representation due to the relational position restrictions, but lacks accuracy due to the large variation in the images. Accuracy will be improved by interleaving the alignment of these features with the knowledge of the expected shape changes. Therefore, these landmark positions give the initialization for this registration process.

II-B. Similarity Measure

The initial landmark estimates, although robust are still liable to have an error of alignment, and are not guaranteed to be placed accurately. As such we need to update them. The crucial aspect is not so much their positions on the image, i.e. where exactly on the bladder the landmark is placed, it is more that the positions of the landmarks in the pre-treatment image correspond to the positions of the landmarks in the post-treatment image. We can look at the correspondence of the landmarks using Mutual Information, or Normalized Mutual Information. In this case, since the images are all T2 weighted MRI, we use Mutual Information, given by:

$$C_{similarity}(A, B) = H(A) + H(B) - H(A, B), \quad (1)$$

to provide a similarity measure between corresponding landmarks points. $H(A)$ and $H(B)$ are the entropies of image segments surrounding the landmark points on the two images and $H(A, B)$ is the joint entropy. We need to apply this similarity measure over a series of scales to give a robust and accurate alignment. Hence the size of the image sub-block used to calculate the Mutual Information will be varied.

II-C. Registration

The method of Thin Plate Splines [6] will be used to register the images. This provides a straightforward method in which to align corresponding landmark points. It is fast to calculate the warp field and as such fast to calculate information about the warp field that can be used in the regularization stage (Sect. II-D).

The Thin Plate Splines will be included in an adaptive registration framework similar to that developed by Park et al. [7]. This algorithm works iteratively over a series scales, searching for the region of maximum misalignment. Park et al. define a mismatch measure, M , based on Mutual Information $C_{similarity}$:

$$M = 1 - \frac{C_{similarity}(A, B)}{\min(H(A), H(B))} \quad (2)$$

This identifies areas of high entropy and low local mis-information which makes for good placement of landmarks. The maximum mismatch can then be found and a landmark is placed and aligned. However the initial problems with this algorithm was that these landmarks are not within the region of interest. Since we have already defined our landmarks and our goal is to align them, we instead use the minimum value of Mutual Information to decide which are our maximum misaligned landmarks, and we can consequently align these.

The alignment is based on a cost function that is due to the similarity between the landmarks, and the anatomy and physiology relationships on the two images. The cost function is minimized using simple gradient descent. We can use this simple method because local minima are unlikely within the small search region around each landmark point. We have already accounted for the large scale deformations by including these particular landmarks in the first place.

The registration operates across a series of scales from coarse to fine. As the scale becomes finer the sub-block size used to calculate the mutual information becomes smaller. The scale is refined when a threshold is met or when no further improvement can be made.

II-D. Regularization

Shape knowledge was used in identifying the initial landmarks and this knowledge needs to be incorporated throughout the registration as well, to ensure a fully simultaneous algorithm, making the most of all the information available.

There are two types of information that can be used. Firstly the anatomy knowledge, which involves information about the relative positions of the images. That is the colorectum is always lower in the image than the bladder. The bone structures will be level assuming the images are rigidly aligned based on the hip positions, the coccyx is along the line perpendicular to that connecting the hips, from the midpoint of the hips and so on. These are included as series of restrictions such as if they are not met then the cost function will increase greatly.

The other type of information that can be used is the physiology. This is the knowledge of how the patient is likely to have changed from one scan to the next. That is the tumor and surrounding area may have contracted considerably, or alternatively there may be little change. Also the bladder may be full in one image, and empty in another and so on. We can represent both the anatomy and the physiology knowledge using a scalar representation of the warp field, the Jacobian. The Jacobian $J(A, B)$ gives an indication as to whether the tissue is expanding or contracting in a particular region [8]. A first estimate of this physiology change can be found by looking at the warp field of the initial landmarks and some calculated landmarks estimating the position of the mesorectal fascia and the colorectum, which will give an impression as to which regions are acting in which way.

A final cost measure of the anatomy and physiology is introduced based on the linear correlation between the expected and updated Jacobian representations:

The two Jacobians are taken to be the two dimensions of a random variable $(J_{initial}(A, B), J_{update}(A, B)) = (X, Y)$, where $J_{update}(A, B)$ is the jacobian calculated from the current updated landmarks. The correlation coefficient, which is represented in the cost function is then:

$$C_{physiology}(A, B) = \frac{\sigma_{XY}}{\sigma_X \sigma_Y} \quad (3)$$

where $\mu_X = E(X)$, $\mu_Y = E(Y)$, $\sigma_X^2 = E([X - \mu_X]^2)$ and $\sigma_Y^2 = E([Y - \mu_Y]^2)$ are the means and variances of the marginal distributions of X and Y , and σ_{XY} is the covariance of X and Y , given by $\sigma_{XY} = E([X - \mu_X][Y - \mu_Y]) = E(XY) - E(X)E(Y)$.

II-E. Final Algorithm

Putting all the landmark detection, adaptive registration and regularization together the new algorithm can be illustrated as in Fig. 2. The algorithm looks very similar to the adaptive registration of Park et al. [7] except for the initialization using the anatomy knowledge and the cost function which also incorporates that knowledge. The cost function to be minimized is

$$C = -C_{similarity} - \lambda C_{physiology}. \quad (4)$$

The choice of λ is important for the implementation of the algorithm as this indicates how much the prior information

```

Do Find rigid features – hips and coccyx
Do Affine registration based on rigid features
Do Find initial estimates of anatomical relational landmarks, and initial
    Jacobian regularizer estimate
For I = large scale to small scale
    Do
        Identify Maximally misaligned landmark using MI
        Optimize Landmark points to minimize cost function
        While Cost function decrease > threshold
    End For

```

Fig. 2. Simultaneous Landmark Detection and Registration

is used over the similarity and vice versa. For $\lambda = 0$ the anatomy and physiology knowledge is not incorporated at all, whereas for much larger values of λ the similarity measure has no effect. We ran the algorithm for large range of λ values. The optimum value of lambda that we chose was $100\sqrt{10}$.

To improve the accuracy of the algorithm further in the mesorectal region of interest some extra landmarks were added within the fat layer. Although they do not necessarily correspond to features or landmarks within the image, they will have a unique pattern due to any lymph nodes, blood vessels or artifacts such as streaking within that region. As such they are useful to align to provide an even more accurate representation of the registration. The additional landmarks are added using the current points that are known such that we know that these landmarks will lie within the region of interest.

III. RESULTS AND DISCUSSION

This algorithm gives a robust estimate of the registration for 10 corresponding pairs of unseen data slices (separate from those used in the training stage). That is, a clinically useful, sensible result is calculated for all cases. The precision of the algorithm was measured using corresponding lymph nodes, and the results can be seen in Table I. Lymph nodes form distinctive landmarks that are unique to each patient. They are present in the mesorectum, which is the region of most clinical interest, and they are the features that clinicians look to compare in the pre and post therapy images. Hence it is crucial for the success of the registration that they are accurately and robustly aligned. However due to their uniqueness in individual patients it is not trivial to use them to drive the registration algorithm themselves. As noted in [3], prior to registration they can be typically misaligned by 21mm.

The algorithm was run using three sub-block sizes for 3 different scales, of 10, 5 and 2 pixels, and a step size of 1 pixel for the gradient descent. λ was chosen to be

Table I. Comparison of the node misalignments (mm) for each of the 10 datasets, running the Park-Meyer algorithm on its own, the Park-Meyer algorithm with shape initialization, and finally using the simultaneous algorithm.

Patient	Park-Meyer	With initialization	Simultaneous
1	8.76	3.22	3.51
2	8.77	5.76	4.45
3	12.74	7.08	1.92
4	8.33	3.58	2.00
5	FAIL	7.01	3.48
6	8.76	3.88	3.48
7	5.06	4.06	3.65
8	FAIL	5.36	3.29
9	FAIL	6.36	5.00
10	7.59	3.77	3.48

$100\sqrt{10}$. This is large due to the relative orders of magnitude of the similarity and regularization measures. The overall mean node misalignment for all 10 data-sets is 3.42mm. Most enlarged lymph nodes are at least 5mm in diameter and hence an error of 3mm is an accurate registration result. All tests were run in 2D, although the method is easily extendable to 3D.

To compare, the adaptive registration algorithm with no shape knowledge input failed on 3 out of the 10 data-sets. That is corresponding lymph nodes could not be identified as they were misaligned by more than 14mm. This failure rate means that this would not be clinically useful. The precision of this algorithm was such that the mean distance between corresponding nodes was 8.6mm. Using the segmentation as an initial alignment, but not interleaving it simultaneously, the algorithm was much more robust and gave a clinically useful result in all cases. However the precision was such that the misalignment of the nodes was 5mm. These comparisons can be seen in Table I and Fig. 3. The points show the reliability, as percentage success over the 10 data-sets, against the precision. The precision is calculated as the average across the data-sets. The standard deviation for the results with just the Park Meyer algorithm is 3.65mm. With the shape initialization only the standard deviation is 2.06mm, and with the simultaneous algorithm, it is 1.61mm.

Although the algorithm is more computationally costly when shape knowledge is incorporated, as there is the extra segmentation stage, the results show that when using this shape knowledge, the registration is 100% reliable on all the data-sets tested to date. Incorporating the shape knowledge into the simultaneous algorithm increases the computation further as the Jacobian is checked at each iteration. However, looking at the increased precision and robustness of the results by incorporating shape knowledge, it can be seen that this compensates for the increased computation.

IV. CONCLUSIONS

We have shown that by introducing a simultaneous registration and landmark detection technique we can provide

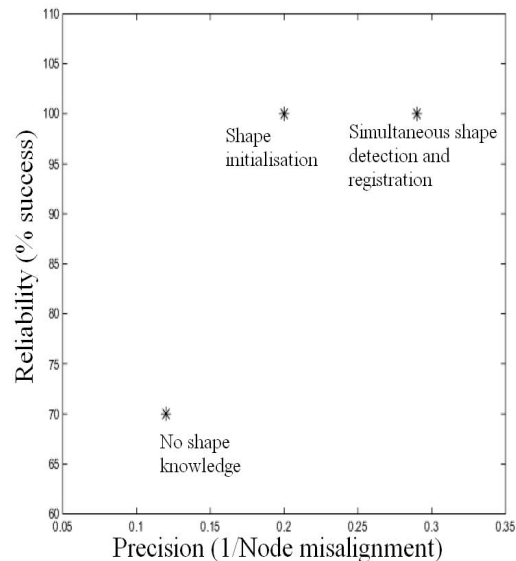


Fig. 3. Reliability and Precision of non-rigid registration algorithms with and without the use of shape knowledge.

an extremely accurate and robust registration of colorectal cancer images pre and post treatment. These are data-sets which have large scale deformations, and cannot be registered using generic 'off the shelf' algorithms.

V. REFERENCES

- [1] S. Bond and M. Brady, "Image analysis for patient management in colorectal cancer," *CARS*, 2005.
- [2] G. Brown, C. Richards, J. Newcombe, N. Dallimore, A. Radcliffe, D. Carey, M. Bourne, and G. Williams, "Rectal carcinoma: Thin-section mr imaging for staging in 28 patients," *Radiology*, vol. 211, pp. 215–222, 1999.
- [3] S. Bond and M. Brady, "Non-rigid registration for colorectal cancer mr images," *CVBIA LNCS 3765*, 2005.
- [4] X. Chen, M. Brady, and D. Rueckert, "Simultaneous segmentation and registration for medical images," *MIC-CAI*, 2004.
- [5] S. Bond, "Forthcoming thesis: Image analysis for patient management in colorectal cancer," 2006.
- [6] F. Bookstein, "Principal warps: Thin-plate splines and the decomposition of deformations," *IEEE PAMI*, vol. 11, pp. 567–585, 1989.
- [7] H. Park, P.H. Bland, K.K. Brock, and C.R. Meyer, "Adaptive registration using local information measures," *MIA*, vol. 8, pp. 465–473, 2004.
- [8] D. Rey, G. Subsol, H. Delingette, and N. Ayache, "Automatic detection and segmentation of evolving processes in 3d medical images: Application to multiple sclerosis.," *IPMI LNCS 1613*, pp. 154–167, 1999.